

Ferromagnetic resonance in uniaxial crystals with cylindrical domain structures

M. A. Sigal

Kiev State University

(Submitted November 24, 1973)

Zh. Eksp. Teor. Fiz. 66, 1762-1776 (May 1974)

A theoretical and experimental study has been made of the resonance absorption caused by uniform precession of the magnetization of the cylindrical domains and of the matrix in a uniaxial crystal, for magnetization perpendicular and parallel to the axis of easy magnetization. Expressions are derived that determine the dependence of external field of the spectrum of characteristic frequencies and of the intensities of the resonance lines. Ferromagnetic resonance in magnetoplumbite crystals has been investigated experimentally by the magnetic-spectra method. The experimental and theoretical results are compared.

INTRODUCTION

The effect of domain structure on ferromagnetic resonance (FMR) in uniaxial crystals was first investigated in^[1], where the model considered was a crystal divided into infinitely thin, plane-parallel layers oppositely magnetized along the axis of easy magnetization (AEM). The spectrum of characteristic frequencies^[1] consists of two branches, whose dependence on the field is determined by the angle between the plane of the boundaries and the external field H , which is perpendicular to the AEM. The frequency spectrum for arbitrary orientation of H with respect to the AEM was calculated in^[2]. In^[3] the equations of motion of the magnetization of a magnetically two-phase system were solved in a Cartesian coordinate system, and the components of the magnetic susceptibility tensor were given in explicit form. Experimentally, the two branches of the resonance frequencies of a crystal with a stripe domain structure (magnetoplumbite) were first measured in^[4] for the case $H \perp$ AEM.

The purpose of the present work is the theoretical and experimental investigation of the FMR of crystals which in the initial state ($H = 0$) have a cylindrical domain structure; the external field is directed perpendicular or parallel to the AEM. FMR in crystals with cylindrical domain structure has not been investigated previously.

In^[5] there was given, without detailed calculation, an expression for the resonance frequency of a single-frequency absorption curve of a crystal in the form of an ellipsoid of revolution, with a cylindrical domain structure, in the special case $H = 0$:

$$\omega_{cd} = \gamma [(H_0 + NM)(H_0 + N_{\text{bound}} M)]^{1/2},$$

whereas experimentally^[6] a two-frequency resonance curve is observed. Such an important difference is probably explained by the fact that in^[5] the dynamic demagnetizing field of the domain boundaries was incorrectly determined.

The basic difference in the formulation of the problem of FMR in uniaxial crystals with plane-parallel and with cylindrical domain structures is connected with the determination of the dynamic demagnetizing field of the domain boundaries, h_{bound} . In the case of the plane-parallel structure, h_{bound} is uniform in each of the two oppositely magnetized groups of domains (provided the width of the domains is much smaller than their other two dimensions). Under the influence of a field perpendicular to the AEM, the magnetic structure of the

crystal is symmetric, and therefore in the total susceptibility of the crystal it is impossible to determine the contribution of each of the magnetic phases.

A crystal in which a cylindrical domain structure has been created consists of two asymmetric oppositely magnetized magnetic phases: the cylindrical domains and the matrix. There is therefore a significant difficulty connected with the determination of h_{bound} inside the cylindrical domains and outside them, in the matrix. If the diameter of the cylindrical domains is much smaller than the thickness of the crystal, one may take h_{bound} to be uniform within the cylindrical domains, treating them as prolate ellipsoids of revolution. Outside the cylinders (in the matrix), h_{bound} is nonuniform and decreases with increase of distance from the axis of the cylinder. The function that describes the distribution of h_{bound} in the matrix depends on the ratio of the diameter of the cylinders to the distance between them, on the type of lattice that the cylindrical domains form, etc. In the present work, the problem of FMR in a crystal with cylindrical domain structure is solved approximately, without allowance for interaction between the cylindrical domains, on the assumption that h_{bound} falls off to zero at a distance from a cylinder that is much smaller than the distance between them; in this approximation, therefore, h_{bound} in the matrix is zero.

SPECTRUM OF CHARACTERISTIC FREQUENCIES AND "SCALAR" SUSCEPTIBILITY

1. External Field Perpendicular to Axis of Easy Magnetization

We consider a uniaxial crystal in the form of an ellipsoid of revolution, whose axis coincides with the AEM and is parallel to the Z axis ($N_x = N_y = N$, $N_z = 4\pi - 2N$). The external field H is directed along the X axis. In the initial state ($H = 0$) the crystal consists of a hexagonal lattice formed by cylindrical domains, whose magnetization M_1 lies along the positive direction of the Z axis. The magnetization M_2 of the crystal matrix is opposite to the magnetization of the cylindrical domains, and $M_1 = M_2 = M/2$. The equilibrium positions of the magnetizations $M_1(\theta_1, \varphi_1)$ and $M_2(\theta_2, \varphi_2)$ in a field H , determined from the condition of a minimum of the free energy, are determined in the case under consideration, just as in the case of a crystal with a stripe domain structure^[1], by the relations

$$\varphi_1 = \varphi_2 = 0, \quad \sin \theta_1 = \sin \theta_2 = \sin \theta = \frac{H}{H_0 + NM}, \quad \theta_1 + \theta_2 = \pi, \quad (1)$$

where $H_a = 2k/M$ (k is the first crystalline-anisotropy constant) and $H < H_a + NM$.

In a Cartesian system, the components of the constant magnetization are connected by the relations^[3]

$$\begin{aligned} M_{1x} = M_{2x} = M_x/2, \quad M_{1y} = M_{2y} = 0, \\ M_{1z} = -M_{2z} = M_z/2, \quad H - N_z M_x = H_{an} M_x / M_z, \quad H_{an} = H_a \cos \theta. \end{aligned} \quad (2)$$

The equations of motion for the magnetizations of the two magnetic phases, in the absence of absorption, will be solved as in reference^[3] in a Cartesian system; in contrast to reference^[1], the natural FMR ($H = 0$) can be obtained as a special case.

In the first approximation, by neglecting quantities of the second order of smallness we have

$$\begin{aligned} dm_1/dt = -\gamma \{ [m_1(H + H_{dem} + H_{an})] + [M_1(h + h_{dem} + h_{1,an} + h_{1,bound})] \}, \\ dm_2/dt = -\gamma \{ [m_2(H + H_{dem} - H_{an})] + [M_2(h + h_{dem} + h_{2,an})] \}. \end{aligned} \quad (3)$$

Here m_1 and m_2 are the alternating magnetizations of the cylindrical domains and of the matrix, respectively; H_{dem} and h_{dem} are the crystal-shape demagnetizing fields induced by the constant and by the alternating magnetizations:

$$H_{dem} = -N(M_{1x} + M_{2x}) \mathbf{x} = -NM_x \mathbf{x}, \quad (4)$$

$$h_{dem} = -[N(m_{1x} + m_{2x}) \mathbf{x} + N_z(m_{1y} + m_{2y}) \mathbf{y} + N_z(m_{1z} + m_{2z}) \mathbf{z}];$$

\mathbf{x} , \mathbf{y} , \mathbf{z} are unit vectors; H_{an} and h_{an} are the constant and the alternating components of the crystalline-anisotropy field,^[3] which depend on the direction of the magnetization in the crystal and are equal to

$$H_{an} = \frac{2K}{M^2} M_z z, \quad h_{1an} = \frac{4K}{M^2} m_{1z} z, \quad h_{2an} = \frac{4K}{M^2} m_{2z} z, \quad (5)$$

$h(h_x, h_y)$ is the external exciting field of frequency ω , which acts in the plane perpendicular to the AEM; $h_{1,bound}$ is the demagnetizing field inside the cylindrical domains, produced by the discontinuity of the alternating magnetization at the domain boundary. On setting $N_{bound} = 2\pi$ for an infinitely long cylinder, we have

$$\begin{aligned} h_{1x,bound} = -2\pi(m_{1x} - m_{2x}), \\ h_{1y,bound} = -2\pi(m_{1y} - m_{2y}). \end{aligned} \quad (6)$$

The basic difference between the equations of motion (3) of a two-phase system of cylindrical domains and a matrix and the equations for a two-phase system of stripe domains^[3] consists in the asymmetry of Eqs. (3) with respect to the demagnetizing field of the domain boundaries, which is a consequence of the geometric asymmetry of such a system. Outside the cylindrical domains, in the approximation adopted, $h_{2,bound} = 0$.

From Eqs. (3) in the case of a thin crystal ($N = 0$, $N_z = 4\pi$), there follows for the frequencies of coupled oscillations the expression

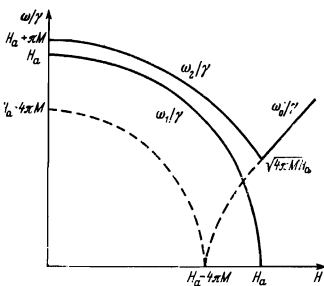


FIG. 1. Spectrum of characteristic frequencies of uniform precession of a uniaxial crystal with a cylindrical domain structure (thin plate) for magnetization in a direction perpendicular to the AEM, calculated by formula (7) for magnetoplumbite; $H_a = 15.3$ kOe, $M = 0.32$ kG. The dotted curve shows the spectrum of a single-domain crystal from [1].

$$\begin{aligned} z_{1,2}^2 = \left(H_a^2 + \pi M H_a + \frac{\pi^2 M^2}{2} \right) - H^2 \left(1 - \frac{\pi M}{H_a} + \frac{\pi^2 M^2}{2 H_a^2} \right) \\ \pm \pi M \left[\left(H_a + \frac{\pi M}{2} \right)^2 - 2 H^2 \left(1 + \frac{\pi^2 M^2}{4 H_a^2} \right) + H^4 \left(\frac{5}{H_a^2} - \frac{\pi M}{H_a^3} + \frac{\pi^2 M^2}{4 H_a^4} \right) \right]^{1/2}. \end{aligned} \quad (7)$$

The expression (7) describes sufficiently accurately the frequency spectrum of a highly anisotropic crystal ($q = 4\pi M/H_a \ll 1$) even when $N \neq 0$.

The spectrum of characteristic frequencies of oscillation of the magnetization of a crystal with cylindrical domain structure (Fig. 1) consists of two branches. With increase of the field H , the low-frequency branch $z_1 = \omega_1/\gamma$ falls to zero at the saturation point $H = H_a$. The high-frequency branch $z_2 = \omega_2/\gamma$ falls to $z_{02} = (4\pi M H_a)^{1/2}$ at the point $H = H_a$. At this point the branches of the characteristic frequencies of saturated ($H \geq H_a$) and unsaturated ($H < H_a$) crystals coincide.

The components of the total alternating magnetization of the crystal are

$$m_x = \chi_{11} h_x + j \chi_{12} h_y, \quad m_y = -j \chi_{21} h_x + \chi_{22} h_y, \quad (8)$$

the tensor components have the form

$$\begin{aligned} \chi_{11} = \frac{MC(z^2 - AB) \cos \theta}{(z^2 - z_1^2)(z^2 - z_2^2)}, \quad \chi_{12} = \frac{MCNz \cos \theta}{(z^2 - z_1^2)(z^2 - z_2^2)}, \\ \chi_{21} = \frac{MANz \cos \theta}{(z^2 - z_1^2)(z^2 - z_2^2)}, \quad \chi_{22} = \frac{MA(z^2 - BC) \cos \theta}{(z^2 - z_1^2)(z^2 - z_2^2)}, \end{aligned} \quad (9)$$

where

$$\begin{aligned} A = H_a + \pi M + 4\pi M \frac{\sin^2 \theta}{\cos^2 \theta}, \quad B = H_a \cos \theta, \quad C = (H_a + \pi M) \cos \theta, \\ n = \pi M \cos \theta, \quad z = \omega/\gamma \end{aligned}$$

(since the exciting field lies in the plane perpendicular to the AEM ($h_z = 0$), the component m_z does not affect the "scalar" susceptibility, and we do not write it down here).

The "scalar" susceptibility χ , defined as the ratio of the projection m_h of the alternating magnetization of the crystal along the direction of the exciting field to the value of the field, is

$$\chi = \frac{m_h}{h} = \frac{mh}{h^2} = \frac{1}{h^2} (\chi_{11} h_x^2 + j \chi_{12} h_x h_y - j \chi_{21} h_x h_y + \chi_{22} h_y^2). \quad (10)$$

We shall consider two special cases:

1) Parallel excitation: $h \parallel H$, $h_x = h$, $h_y = 0$. In this case

$$\chi_{||} = \chi_{11}. \quad (11)$$

2) Perpendicular excitation: $h \perp H$, $h_x = 0$, $h_y = h$. In this case

$$\chi_{\perp} = \chi_{22}. \quad (12)$$

For analysis of the dependence of the intensities of the resonance peaks on the external biasing field H , it is convenient to represent the two-frequency curves (11) and (12) as a superposition of two single-frequency curves. On allowing for absorption, as usual, by introduction of a complex frequency $\omega - j\omega_r$, we obtain for the frequency dependence of the imaginary part of the scalar susceptibility the expressions

$$\chi_{||}'' = \chi_{11}'' + \chi_{21}'' = \frac{2\gamma^2 \omega_r MC (\gamma^2 AB - \omega_r^2) \cos \theta}{[(\omega^2 - \omega_r^2)^2 + 4\omega^2 \omega_r^2] (\omega_1^2 - \omega_2^2)} - \frac{2\gamma^2 \omega_r MC (\gamma^2 AB - \omega_r^2) \cos \theta}{[(\omega^2 - \omega_r^2)^2 + 4\omega^2 \omega_r^2] (\omega_2^2 - \omega_1^2)}, \quad (13)$$

$$\chi_{\perp}'' = \chi_{12}'' + \chi_{22}'' = -\frac{2\gamma^2 \omega_r MA (\gamma^2 BC - \omega_r^2) \cos \theta}{[(\omega^2 - \omega_r^2)^2 + 4\omega^2 \omega_r^2] (\omega_1^2 - \omega_2^2)} - \frac{2\gamma^2 \omega_r MA (\gamma^2 BC - \omega_r^2) \cos \theta}{[(\omega^2 - \omega_r^2)^2 + 4\omega^2 \omega_r^2] (\omega_2^2 - \omega_1^2)}. \quad (14)$$

We shall determine the dependence on external field of the relative intensity $K(H)$ of the low-frequency and of the high-frequency maxima of the absorption curves, under conditions of parallel ($\chi''_{\parallel \max}(\omega = \omega_1)$, $\chi''_{\parallel \max}(\omega = \omega_2)$) and perpendicular ($\chi''_{1 \perp \max}(\omega = \omega_1)$, $\chi''_{2 \perp \max}(\omega = \omega_2)$) excitation, on the assumption that the relaxation frequency ω_r does not depend on the external field. We have

$$K_{\parallel}(H) = \frac{\chi''_{\parallel \max}(H)}{\chi''_{\parallel \max}(0)} = \frac{\gamma(\gamma^2 AB - \omega_1^2)(2H_a + \pi M)}{(\omega_2^2 - \omega_1^2)\omega_1} \cos^2 \theta, \quad (15)$$

$$K_{2\parallel}(H) = \frac{\chi''_{2\parallel \max}(H)}{\chi''_{2\parallel \max}(0)} = \frac{\gamma(\gamma^2 AB - \omega_2^2)(2H_a + \pi M)}{(\omega_1^2 - \omega_2^2)\omega_2^2} \cos^2 \theta, \quad (16)$$

$$K_{1\perp}(H) = \frac{\chi''_{1\perp \max}(H)}{\chi''_{1\perp \max}(0)} = \frac{\gamma(\gamma^2 BC - \omega_1^2)(2H_a + \pi M) [(H_a + \pi M) \cos^2 \theta + 4\pi M \sin^2 \theta]}{(\omega_2^2 - \omega_1^2)\omega_1 (H_a + \pi M)} \quad (17)$$

$$K_{2\perp}(H) = \frac{\chi''_{2\perp \max}(H)}{\chi''_{2\perp \max}(0)} = \frac{\gamma(\gamma^2 BC - \omega_2^2)(2H_a + \pi M) [(H_a + \pi M) \cos^2 \theta + 4\pi M \sin^2 \theta]}{(\omega_1^2 - \omega_2^2)\omega_2 (H_a + \pi M)} \quad (18)$$

With approach to saturation, the intensities of both peaks in the case of parallel excitation approach zero. For perpendicular excitation near saturation, the intensity of the low-frequency peak approaches zero. At the saturation point, only the intensity of the high-frequency peak $K_{2\perp}(H_a)$ differs from zero. It is interesting that in this case $K_{2\perp}(H_a) = K_{2\perp}(0)$; for $H > H_a$ this peak is the FMR curve of a saturated specimen.

2. External Field Parallel to Axis of Easy Magnetization

In the previously considered case $H \perp$ AEM, the static magnetization vectors of the magnetic phases (cylindrical domains and matrix) deviate from their equilibrium values at $H = 0$, whereas the volumes of the magnetic phases remain unchanged. In the case $H \parallel$ AEM, magnetization of the crystal is accomplished by displacement of the domain boundaries. The static values of the magnetization of the cylindrical domains (M_1) and the matrix (M_2) are determined from the relations

$$\begin{aligned} M_{1z} = M_1 = H/2N_z + M/2, \quad M_{1x} = M_{1y} = 0, \\ M_{2z} = M_2 = H/2N_z - M/2, \quad M_{2y} = M_{2x} = 0, \\ M_1 + M_2 = H/N_z, \quad M_1 - M_2 = M. \end{aligned} \quad (19)$$

From (19) it is evident that when a positive external field is directed along the direction of magnetization of the cylindrical domains ($H \parallel M_1$), M_1 increases with increase of the field, whereas the magnetization M_2 of the matrix decreases, according to a linear law.

The spectrum of characteristic frequencies and the components of the susceptibility tensor will be determined again by solution of Eqs. (3), where in contrast to (4) and (5)

$$H_{\text{dem}} = -N_z(M_1 + M_2)z, \quad H_{\text{an}} = H_a z, \quad H = Hz. \quad (20)$$

In the case of a thin crystal

$$z_{1,2}^2 = 1/2(L^2 + 2RH_a) \pm 1/2L(L^2 + 4RH_a)^{1/2}, \quad (21)$$

where $R = H_a + \pi M + H/4$, $L = \pi M + H/4$, whence

$$z_1 = \omega_1/\gamma = H_a, \quad z_2 = \omega_2/\gamma = H_a + \pi M + H/4. \quad (22)$$

The frequency spectrum consists of two branches. The frequency of the low-frequency branch is independent of the external field and equal to the natural FMR fre-

quency in the crystalline-anisotropy field. The high-frequency branch changes linearly with the field, and consequently the position of this branch depends on the sign of H ; that is, on the orientation of the external field with respect to the magnetization of the cylindrical domains.

The components of the alternating magnetization of the crystal are

$$m_x = \chi_{11} h_x + j\chi_{12} h_y, \quad m_y = -j\chi_{21} h_x + \chi_{22} h_y, \quad (23)$$

where

$$\begin{aligned} \chi_{11} = \chi_{22} &= \frac{4\pi R^2 H_a M - LRH_a H + 4\pi z^2 RM}{4\pi(z^2 - z_1^2)(z^2 - z_2^2)}, \\ \chi_{12} = \chi_{21} &= \frac{z(HL^2 + H_a RH - z^2 H - 4\pi RLM)}{4\pi(z^2 - z_1^2)(z^2 - z_2^2)}. \end{aligned}$$

We shall determine the "scalar" susceptibility χ of the crystal:

$$\chi = (mh) / h^2 = \chi_{11}. \quad (24)$$

On taking into account the dependence (21) of R and L on H , we get

$$\chi = \frac{\gamma\omega_2(\gamma^2 \Pi - M\omega^2)}{(\omega^2 - \omega_1^2)(\omega^2 - \omega_2^2)}, \quad \Pi = \pi H_a \left(M^2 - \frac{H^2}{16\pi^2} \right) + MH_a^2. \quad (25)$$

On representing the two-frequency dependence (25) in the form of a superposition of two single-frequency resonance curves and on allowing for absorption, we get

$$\begin{aligned} \chi'' = \chi_1'' + \chi_2'' &= \frac{2\gamma\omega\omega_1\omega_2(\gamma^2 \Pi - M\omega_1^2)}{[(\omega^2 - \omega_1^2)^2 + 4\omega^2\omega_1^2](\omega_2^2 - \omega_1^2)} \\ &+ \frac{2\gamma\omega\omega_1\omega_2(\gamma^2 \Pi - M\omega_2^2)}{[(\omega^2 - \omega_2^2)^2 + 4\omega^2\omega_2^2](\omega_1^2 - \omega_2^2)}. \end{aligned} \quad (26)$$

The reduced intensities $K_1(H)$ and $K_2(H)$ of the resonance maxima have the form

$$K_1(H) = \frac{\chi_1'' \max(H)}{\chi'' \max(0)} = \frac{(2H_a + \pi M)(H_a + \pi M + H/4)(4\pi M - H)}{\pi M(H_a + \pi M)(H + 4\pi M + 8H_a)}, \quad (27)$$

$$K_2(H) = \frac{\chi_2'' \max(H)}{\chi'' \max(0)} = \frac{(2H_a + \pi M)(H + 4\pi M)}{\pi M(H + 4\pi M + 8H_a)}. \quad (28)$$

From (27) and (28) it is evident that in the case of a highly anisotropic crystal ($\epsilon = 4\pi M/H_a \ll 1$), there is an almost linear dependence $K_2(H)$, differing little from the dependence $M_1(H)$ of (19); that is, the intensity of the high-frequency peak is almost proportional to the magnetization of the cylindrical domains.

There is an analogous relation between the intensity of the low-frequency peak and the magnetization of the matrix. From what has been said it may be supposed that excitation of the high-frequency maximum is caused chiefly by precession of the magnetization of the cylindrical domains, and of the low-frequency by precession of the magnetization of the matrix. Along with this, it follows from (3) that the precessions of the magnetizations of both magnetic phases are coupled oscillations. In order to determine the character of this coupling and its dependence on the external field, it is necessary to investigate the contribution to the absorption curve of the whole crystal from the absorption of each of its magnetic phases separately.

The system (3) in the variables m_1 and m_2 takes the form, in the case of a thin crystal,

$$\begin{aligned} izm_{1x} + Rm_{1y} - Lm_{2y} &= M_1 h_y, \\ -Rm_{1x} + izm_{1y} + Lm_{2x} &= -M_1 h_x, \\ izm_{2x} - H_a m_{2y} = M_2 h_y, \quad H_a m_{2x} + izm_{2y} &= -M_2 h_x. \end{aligned} \quad (29)$$

When $L = 0$ the system (29) breaks up into two pairs of

independent equations. The first and second determine the high-frequency peak, with frequency $\omega_2 = \gamma R = \gamma(H_a + \pi M + H/4)$, whose intensity depends only on M_1 (the magnetization of the cylindrical domains). The third and fourth determine the low-frequency peak $\omega_1 = \gamma H_a$, with intensity dependent only on M_2 (the magnetization of the matrix). Since $L \neq 0$ for $|H| < 4\pi M$, in the range in which domain structure exists the oscillations of the two magnetic phases are coupled.

The characteristic frequencies determined by solution of the system (29) coincide with (21). The components of alternating magnetization of the cylindrical domains, m_1 , and of the matrix, m_2 , are

$$\begin{aligned} m_{1x} &= \chi_{11}^{(1)} h_x + j\chi_{12}^{(1)} h_y, & m_{1y} &= -j\chi_{21}^{(1)} h_x + \chi_{22}^{(1)} h_y, \\ m_{2x} &= \chi_{11}^{(2)} h_x + j\chi_{12}^{(2)} h_y, & m_{2y} &= -j\chi_{21}^{(2)} h_x + \chi_{22}^{(2)} h_y, \end{aligned} \quad (30)$$

where

$$\begin{aligned} \chi_{11}^{(1)} &= \chi_{22}^{(1)} = \frac{1}{\Delta} (Q - Sz^2), & \chi_{12}^{(1)} &= \chi_{21}^{(1)} = \frac{z}{\Delta} (T - M_1 z^2), \\ \chi_{11}^{(2)} &= \chi_{22}^{(2)} = \frac{M_2 H_a}{\Delta} (z^2 - R^2) = \frac{M_2 H_a}{z^2 - H_a^2}, \\ \chi_{12}^{(2)} &= \chi_{21}^{(2)} = \frac{M_2 z}{\Delta} (R^2 - z^2) = -\frac{zM_2}{z^2 - H_a^2}, \\ Q &= R(M_1 H_a^2 - M_2 L H_a), & S &= M_1 R - M_2 L, \\ T &= M_1 H_a^2 + M_2 L^2, & \Delta &= (z^2 - H_a^2)(z^2 - z_2^2). \end{aligned}$$

The "scalar" susceptibilities due to the magnetization precessions of the cylindrical domains ($\chi^{(1)}$) and of the matrix ($\chi^{(2)}$) have the form

$$\chi^{(1)} = (\mathbf{m}, \mathbf{h})/h^2 = \chi_{11}^{(1)}, \quad \chi^{(2)} = (\mathbf{m}, \mathbf{h})/h^2 = \chi_{11}^{(2)}. \quad (31)$$

On representing the resonance curves $\chi^{(1)}$ and $\chi^{(2)}$ as the sums of two single-frequency curves, we get

$$\begin{aligned} \chi^{(1)} &= \chi_1^{(1)} + \chi_2^{(1)} = \frac{\Phi_1}{z^2 - H_a^2} + \frac{\Phi_2}{z^2 - z_2^2}, \\ \chi^{(2)} &= \chi_1^{(2)} = \frac{M_2 H_a}{z^2 - H_a^2}, \quad \chi_2^{(2)} = 0, \end{aligned} \quad (32)$$

where

$$\Phi_1 = \frac{Q - SH_a^2}{H_a^2 - z_2^2}, \quad \Phi_2 = \frac{Q - Sz_2^2}{z_2^2 - H_a^2}.$$

From (32) follows the important conclusion that the precession of the magnetization of the cylindrical domains excites both modes, a high-frequency and a low-frequency, whereas the precession of the magnetization of the matrix excites only a low-frequency peak. As a parameter that describes the degree of coupling between the two modes of precession of the cylindrical domains, we may take the ratio P of the intensity of the "foreign" low-frequency mode to the intensity of the "domestic," i.e., high-frequency mode:

$$P = \frac{\chi_1^{(1) \max}}{\chi_2^{(1) \max}} = \frac{\Phi_1}{\Phi_2} = \frac{1/2 H_a (4\pi M - H)}{(H_a + \pi M)(4H_a + 4\pi M + H)} \quad (33)$$

It is obvious that the degree of coupling for oscillations of the magnetization of the matrix is zero.

The intermode coupling decreases almost linearly (Fig. 2) with increase of the field from $H = -4\pi M$ to $H = 4\pi M$ in crystals with large anisotropy ($q < 1$), since the relative volume of the crystal occupied by cylindrical domains increases. The coupling also decreases with increase of the anisotropy of the crystal, and for $q \ll 1$ the value of P is proportional to q . In the case of magnetoplumbite ($q = 0.263$) at $H = 0$, $P = 0.029$, and therefore it may be stated with a sufficient degree of accuracy that the high-frequency peak is excited by precession of the magnetization of the cylindrical domains,

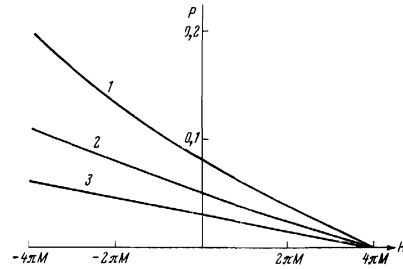


FIG. 2. Dependence upon the external field of the intermode coupling parameter P for precession of the magnetization of the cylindrical domains. Curves constructed according to formula (33): 1, for $q = 1$; 2, for $q = 0.5$; 3, for magnetoplumbite, $q = 0.263$.

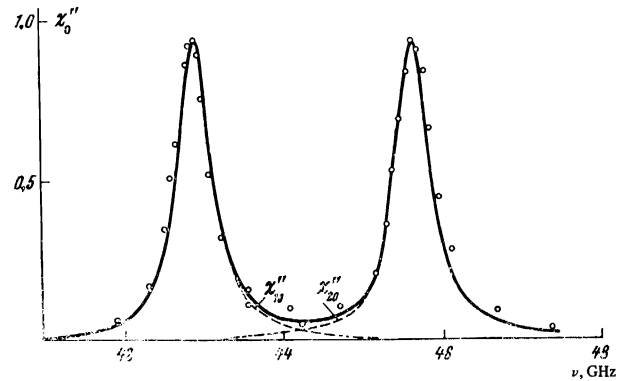


FIG. 3. Spectrum of the "Scalar" magnetic susceptibility of a magnetoplumbite crystal with cylindrical domain structure in the absence of an external field ($H = 0$). Solid curve: frequency dependence of the imaginary part of the susceptibility, χ''_0 , calculated by formula (35). Dotted curve: χ''_{10} and χ''_{20} . Experimental points obtained from measurements on a crystal with $d = 0.044$ mm.

the low-frequency by precession of the magnetization of the matrix.

EXPERIMENTAL RESULTS AND DISCUSSION

1. Natural Ferromagnetic Resonance

The characteristic frequencies and the absorption curve for natural ($H = 0$) FMR of a uniaxial crystal with a cylindrical domain structure (thin crystal) are obtained from one of the expressions (7), (21) and (13), (14), (26), respectively, for the special case $H = 0$:

$$\omega_{10} = \gamma H_a, \quad \omega_{20} = \gamma(H_a + \pi M); \quad (34)$$

$$\begin{aligned} \chi''_0 &= \chi''_{10} + \chi''_{20} = \frac{2\gamma^2 \omega \omega_r (H_a + \pi M) M H_a}{[(\omega^2 - \gamma^2 H_a^2)^2 + 4\omega^2 \omega_r^2] (2H_a + \pi M)} \\ &+ \frac{2\gamma^2 \omega \omega_r M (H_a + \pi M)^2}{\{[\omega^2 - \gamma^2 (H_a + \pi M)^2]^2 + 4\omega^2 \omega_r^2\} (2H_a + \pi M)}. \end{aligned} \quad (35)$$

The intensity is the same for both resonance lines and is

$$\chi''_{10 \max}(\omega = \omega_1) = \chi''_{20 \max}(\omega = \omega_2) = \frac{\gamma M (H_a + \pi M)}{2\omega_r (2H_a + \pi M)}. \quad (36)$$

In constructing the theoretical curve for χ''_0 (Fig. 3) we adopted the following values of the parameters: $H_a = 15.3$ kOe, $M = 0.32$ kG, $\omega_r = 2\pi \cdot 0.25$ GHz. The crystalline-anisotropy field H_a and the relaxation frequency ω_r were determined from the experimental dependence of $\chi''_0(\omega)$ on frequency and the half-width of the low-frequency peak. Since the half-width of the absorption curves is significantly smaller than the frequency interval, $\omega_r \ll \Delta\omega = \omega_2 - \omega_1$, the intensity of the low-

frequency peak coincides with the intensity of the absorption curve of the specimen, χ_0'' , at the frequency $\omega = \omega_1$, i.e. $\chi_0''(\omega = \omega_1) = \chi_0'' \max$, and the intensity of the high-frequency with the intensity χ_0'' at the frequency $\omega = \omega_2$, i.e. $\chi_0''(\omega = \omega_2) = \chi_0'' \max$.

The imaginary part of the "scalar" magnetic susceptibility of the magnetoplumbite crystal was measured by the waveguide method in the thin-specimen approximation:

$$\chi'' = \frac{\lambda_q}{8\pi^2 d} \frac{1}{r}; \quad (37)$$

here λ_q is the wavelength in the waveguide, d is the thickness of the crystal, and r is the standing-wave ratio of the loaded line.

A monocrystalline plate with its AEM perpendicular to the basal plane, filling the cross section of the waveguide, was glued on a cleavage plane to a short-circuiting plate, and then was ground and polished to the necessary thickness. In the choice of thickness we started from the fact that in crystals with $d > 50 \mu\text{m}$, along with the basic structure of stripe or cylindrical domains in the volume of the crystal, there is a complicated surface structure of wedge-shaped domains, with which is associated the excitation of nonuniform types of precession^[7] that hamper the analysis of the magnetic spectra. With decrease of thickness, at $d < 50 \mu\text{m}$ the domain structure simplifies and the conditions for observation of FMR improve; but at small thicknesses, $d < 10 - 15 \mu\text{m}$, the sensitivity of the method becomes insufficient. The measurements were made on a crystal with $d = 44 \mu\text{m}$.

It is well known^[8] that in a thin crystal in the remanent state of magnetization after application of a saturating field at an angle $\theta \approx 90^\circ$ to the AEM, there occurs a magnetic structure consisting of a hexagonal lattice of cylindrical domains. The effect of a domain structure corresponding to variable θ , $\theta < 0 < 90^\circ$, on natural FMR has been investigated by us experimentally, and the results will be presented in another paper.

The optimum conditions for production of cylindrical domains correspond to $\theta \approx 87 - 88^\circ$. The experimental results in Fig. 3 were obtained on a plate magnetized with $\theta = 87.5^\circ$. The agreement of the experimental data with the theoretical curve is good. It must be remarked that with the thickness chosen, the plate may be considered "thin," since $NM \ll H_a$, but it is nevertheless sufficiently "thin" so that we may set $N_{\text{bound}} = 2\pi$ in equation (3).

Actually, at $d = 44 \mu\text{m}$ the ratio of the height of the cylinder to its diameter $\approx 7^{[9]}$, and N_{bound} is about 4% less than 2π . Decrease of the demagnetizing factor of the boundaries of the cylindrical domains of the real crystal as compared with the idealized model should lead to a corresponding drawing together of the resonance peaks.

Our measurements (Fig. 3) do not enable us to observe a frequency shift of the χ_0'' curve, perhaps because of the relatively wide resonance curves of magnetoplumbite.

2. Ferromagnetic Resonance with Crystal Magnetization Perpendicular to AEM

FMR in uniaxial crystals with cylindrical domain structure was investigated by the method of magnetic

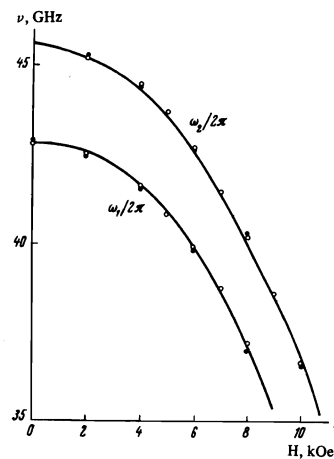


FIG. 4. Dependence of the resonance frequencies of a uniaxial crystal with cylindrical domain structure on an external field $H \perp$ AEM. Solid lines—two branches of the characteristic frequencies, calculated by formula (7). \circ —experimental data obtained under conditions of perpendicular excitation ($h \perp H$). \bullet —parallel excitation ($h \parallel H$).

spectra (MS). In the case of unsaturated crystals, this method has a number of important advantages as compared with the method in which the external field passes through resonance at a fixed frequency, and which is usually applied at fields at which there is no domain structure.

First, in the MS method there acts on the specimen a constant field of fixed value, which forms a static magnetic structure in the crystal, and this structure is probed by an alternating field of very small intensity, whereas the action of a changing external field at fixed frequency is connected with a rotation of M_1 and M_2 ($H \perp$ AEM) or a change of their magnitudes ($H \parallel$ AEM) on passage through resonance. Second, the half-width of the absorption curve measured on the basis of the field,

$$|\Delta H| = \omega_r / \gamma \dot{z}(H) \quad (38)$$

at constant ω_r depends on H because of differing slope of the $z(H)$ curves (Fig. 1). At small values of the magnetizing field, an appreciable increase of ΔH will be observed because of the small value of $\dot{z}(H)$.

Two series of magnetic spectra were measured at fixed values of the magnetizing field H over the field interval from zero to 10 kOe. The range of frequencies used was bounded from below by frequency $\omega = 2\pi \cdot 36.0$ GHz, and therefore the region close to saturation was not investigated. For $H \geq 9$ kOe only the high-frequency peak was measured. The spectrum of the crystal in the initial state ($H = 0$) is given in Fig. 3. Absorption curves were measured with different mutual orientations of the exciting field h and the static field H . In Fig. 4 the two branches of the characteristic frequencies, calculated by formula (7) ($H_a = 15.3$ kOe, $M = 0.32$ kG), are compared with experimental data. Excitation of each of the resonance modes of a crystal with cylindrical domain structure is not connected with a definite orientation of h with respect to H , and therefore, as was to be expected, the resonance frequencies measured under conditions of perpendicular ($h \perp H$) and parallel ($h \parallel H$) excitations practically coincide (the difference is less than the half-width of the absorption curve) and fit the theoretical curve well.

The greatest deviation of the measured frequencies from the theoretical curve does not exceed 0.5%. The good agreement of theory with experiment over the whole range of fields, up to $H \approx 0.7 H_a$, is an indirect corroboration of the stability of the initial cylindrical domain structure in fields below the critical field H_{cr} , known from direct observations of the domain structure

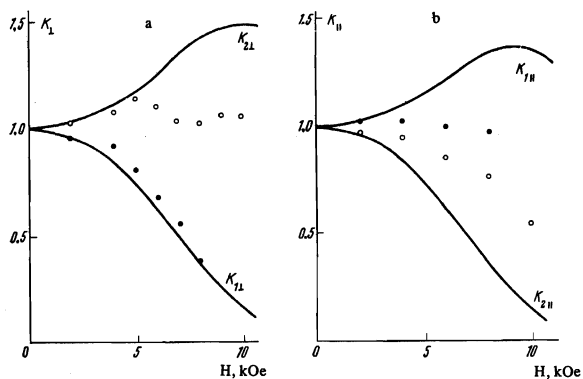


FIG. 5. Dependence of reduced intensity of the resonance lines on an external field $H \perp$ AEM: a—perpendicular excitation; b, parallel excitation. Solid lines—calculated by formulas (15)-(18): K_1 —reduced intensity of the low-frequency peak; K_2 —of the high-frequency peak; ●—experimental values of reduced intensities of the low-frequency peaks; ○—of the high-frequency peaks.

by the Faraday method^[10]. In the case $H \perp$ AEM, $H_{cr} = H_a$. At the same time, such good agreement is unexpected in view of the very considerable approximation $h_{2\text{bound}} = 0$.

We shall consider the experimental and theoretical dependences of the reduced intensities (Fig. 5). Under conditions of perpendicular excitation (Fig. 1a), the intensities of the low-frequency peaks agree quite well with theory, but the intensity of the high-frequency peaks agrees with the theoretical curve only in the low-field range $H < 5$ kOe; with increase of field, the disagreement increases abruptly.

Under conditions of parallel excitation (Fig. 5b), only the intensity of the high-frequency peaks correlates qualitatively with the theoretical curve $K_{2\parallel}$. It is interesting to note that for perpendicular and parallel excitation (Fig. 5b) the theoretical curves whose intensity increases with H deviate from the experimental data more than do the curves whose intensity decreases with increase of H . Comparison of the theoretical and experimental results on resonance frequencies and intensities leads us to surmise that neglect of $h_{2\text{bound}}$ is important in the determination of intensities and unimportant in the determination of the spectrum of characteristic frequencies.

3. Ferromagnetic Resonance with Magnetization Parallel to AEM

FMR with parallel magnetization holds special interest because of the fact that these are the magnetization conditions for operation of the uniaxial crystals with cylindrical domain structure that are used as material for the construction of magnetic memory elements. In the initial state ($H = 0$) these crystals have a stripe-domain structure. A stable cylindrical-domain structure exists only in a relatively small range of external biasing fields, close to saturation; the direction of the magnetization of the cylindrical domains is opposite to the direction of the external field. In the magnetoplumbite plates investigated here, a stable cylindrical-domain structure is realized both in the state of remanent magnetization and under the action of an external field that brings the crystal to saturation, in the direction coinciding with that of the magnetization of the cylindrical domains and in the opposite direction.

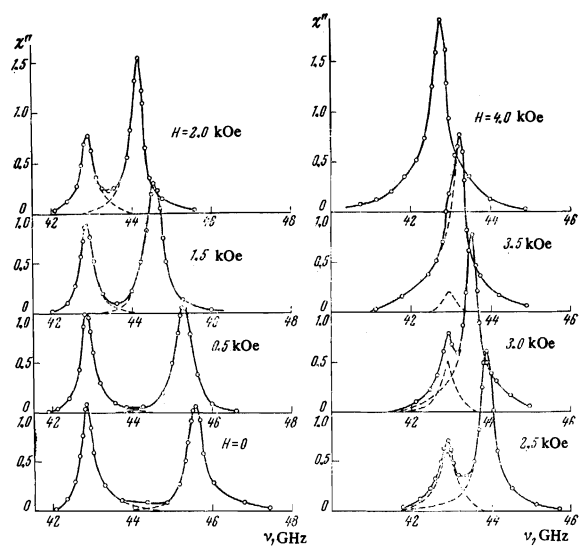


FIG. 6. Spectra of the imaginary part of the magnetic susceptibility of a magnetoplumbite crystal, measured at various values of a field $H \parallel$ AEM. The direction of the external field coincides with the direction of the magnetization of the cylindrical domains ($H \parallel M_1$); $d = 36$ μm . The dotted line shows $\chi''_1 \text{ expt}$ and $\chi''_2 \text{ expt}$.

Figure 6 shows the spectra of the imaginary part of the scalar magnetic susceptibility of a monocrystalline plate of magnetoplumbite ($d = 36$ μm , $\omega_r = 2\pi \cdot 0.21$ GHz, $H_a = 15.3$ kOe, $M = 0.32$ kG). The initial state ($H = 0$) was obtained after saturation at angle $\theta = 87.5^\circ$. The spectra were measured under the action of an external field whose direction coincided with that of the magnetization of the cylindrical domains ($H \parallel M_1$). A series of spectra was also obtained in the case in which the external field was opposite to this direction ($H \parallel M_1$). The orientation of the external field with respect to the magnetization of the cylindrical domains was determined on the basis of the fact that the direction of this magnetization in the remanent-magnetization state^[8] is opposite to the direction of the projection of the saturating field along the normal to the surface of the plate.

Overlapping of the resonance lines, which is appreciable when $\omega_2 - \omega_1 \approx \omega$, is observed for magnetization of the crystal in the direction coinciding with the direction of the magnetization of the cylindrical domains ($H \parallel M_1$, Fig. 6). For this reason the measured intensity of the low-frequency peak, $\chi''(\omega_1)$, is found to be larger than the value of $\chi''_1 \text{ max}$. For comparison with the theoretical curve, we attempted to separate χ''_1 from the total absorption curve of the crystal in the following manner. The χ''_2 curve was completed in such a way that its low-frequency slope was continued symmetrically to its high frequency, whereas χ''_1 was constructed as the difference of the experimental curves χ'' and χ''_2 (dotted line in Fig. 6).

The resonance-frequency spectrum is shown in Fig. 7. The resonance frequency of the low-frequency peak, excited chiefly by precession of the magnetization of the matrix of the crystal, is constant over a broad interval of external fields from zero to saturation, except for a region close to saturation in the direction opposite to the magnetization of the cylindrical domains. The region close to saturation requires special treatment. The experimental values of the resonance frequencies of the high-frequency peak, whose excitation is caused

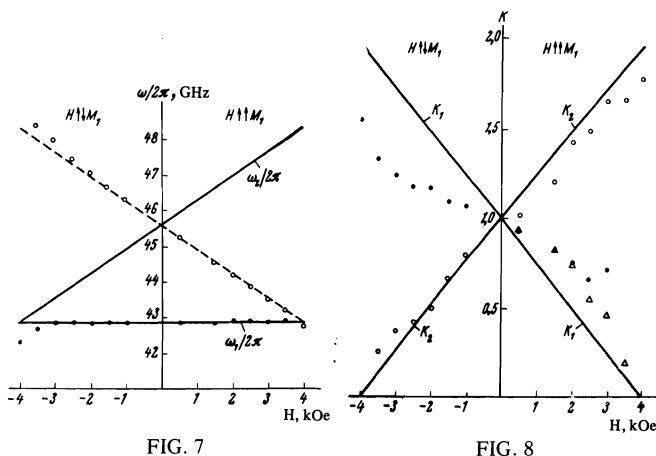


FIG. 7

FIG. 7. Dependence of resonance frequencies of a uniaxial crystal with cylindrical domain structure of an external field $H \parallel \text{AEM}$. Solid lines constructed according to formula (22); $H_a = 15.3$ kOe, $M = 0.32$ kG. In the range of positive values of H , the external field is along the magnetization of the cylindrical domains; in the range of negative values, opposite to it. Experimental points: \bullet —for the low-frequency peak; \circ —for the high-frequency peak. The dotted line shows the curve symmetric to the curve $\omega_2/2\pi$ with respect to the frequency axis.

FIG. 8. Dependence of reduced intensities of resonance lines of a uniaxial crystal with cylindrical domain structure on external field for $H \parallel \text{AEM}$. Solid lines: theoretical curves for the low-frequency (K_1) and high-frequency (K_2) resonance peaks, calculated by formulas (27) and (28). Experimental points: \bullet —for the low-frequency peak; \circ —for the high-frequency peak; \triangle —for the low-frequency peak, constructed with allowance for overlapping of the resonance curves.

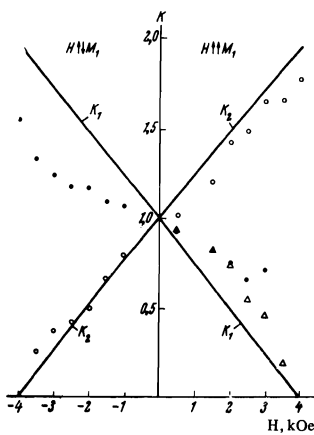


FIG. 8

by precession of the magnetization of the cylindrical domains, are characterized by a linear dependence on external field, except for a region close to saturation with $H \parallel M_1$ (just as in the case of $\omega_1(H)$ for $H \parallel M_1$). But the fact is perplexing that the experimental data fit well the straight line $\omega_2' = \gamma(H_a + \pi M - H/4)$ (dotted line in Fig. 7), which is symmetric to the theoretical straight line $\omega_2(H)$.

We shall consider the effect of an external field on the intensity of the resonance peaks. From (27) and (28) it follows that on magnetization of the crystal in the direction $H \parallel M_1$, the intensity of the high-frequency peak increases, while that of the low-frequency decreases. If the crystal is highly anisotropic, $q = 4\pi M/H_a \ll 1$, the dependence of the intensity of both curves on H is linear. In the case of magnetoplumbite ($q = 0.263$) the reduced intensities $K_1(H)$ (27) and $K_2(H)$ (28) are nearly linear; see Fig. 8.

In Fig. 8 is seen also the qualitative agreement of the experiment with theory. Actually, as was to be expected, with increase of a field ($H \parallel M_1$) the magnetization of the cylindrical domains (19) increases, and as a consequence of this the measured intensity of the high-fre-

quency ("cylindrical") peak increases; on the other hand, with increase of a field ($H \parallel M_1$) the magnetization of the cylindrical domains decreases, and consequently the intensity of the high-frequency peak decreases. An analogous discussion can be given for the intensity of the low-frequency ("matrix") peak. In comparison of the experimental data with the calculated curves, however, it must be remembered that for $H \parallel M_1$ the resonance lines draw together (Fig. 6), and in consequence of their overlapping $\chi''(\omega_1) > \chi''(\omega_2)$; this inequality becomes greater with approach to saturation. The experimental points constructed in Fig. 8 with allowance for overlapping of the resonance curves agree qualitatively with the calculation.

It must be remarked that the measured intensity of the high-frequency resonance agrees appreciably better with the theoretical curve than does the intensity of the low-frequency resonance. This is perhaps explained by the fact that the precession of the magnetization of the matrix makes no contribution to the susceptibility of the high-frequency ("cylindrical") peak, $\chi_2^{(2)} = 0$, and therefore the error due to the approximation $h_2 \text{ bound} = 0$ is unimportant; whereas the error due to this approximation can be very important in the determination of the low-frequency ("matrix") peak, which is almost completely determined by precession of the magnetization of the matrix (in the case $H = 0$, $\chi_1^{(2)}/(\chi_1^{(1)} + \chi_1^{(2)}) = 0.97$).

The authors thank A. V. Zagoruiko and E. I. Petropavlovskii for help in the taking of the measurements.

¹J. Smit and H. G. Beljers, Philips Res. Rep. 10, 113 (1955).

²K. B. Vlasov and L. G. Onoprienko, Fiz. Met. Metalloved. 15, 45 (1963) [Phys. Met. Metallogr. 15, No. 1, 41 (1963)].

³J. Fiksa, J. Phys. Soc. Jap. 29, 1152 (1970).

⁴M. A. Sigal and V. P. Cherevko, Fiz. Tverd. Tela 14, 38 (1972) [Sov. Phys.-Solid State 14, 30 (1972)].

⁵L. G. Onoprienko, O. I. Shiryayeva, and Ya. S. Shur, Izv. Akad. Nauk SSSR Ser. Fiz. 28, 504 (1964) [Bull. Acad. Sci. USSR Phys. Ser. 28, 413 (1964)].

⁶M. A. Sigal, Zh. Eksp. Teor. Fiz. Pis'ma Red. 17, 563 (1973) [JETP Lett. 17, 403 (1973)].

⁷M. A. Sigal, Fiz. Tverd. Tela 15, 1410 (1973) [Sov. Phys.-Solid State 15, 955 (1973)].

⁸J. Kaczér and R. Gemperle, Czech. J. Phys. B11, 510 (1961).

⁹D. J. Craik and P. V. Cooper, J. Phys. D. (Appl. Phys.) 5, L37 (1972).

¹⁰H. Kojima and K. Goto, J. Appl. Phys. 36, 536 (1965).

Translated by W. F. Brown, Jr.